Ordered magnetic and quadrupolar states under hydrostatic pressure in orthorhombic $PrCu_2$

T. Naka,[1,*] L. A. Ponomarenko,[2] A. de Visser,[2] A. Matsushita,[1] R. Settai,[3] and Y. Ōnuki[3]
[1]*Materials Engineering Laboratory, National Institute of Materials Science, Tsukuba, Ibaraki 305-0047, Japan*
[2]*Van der Waals-Zeeman Institute, University of Amsterdam, Valckenierstraat 65, 1018 XE, Amsterdam, The Netherlands*
[3]*Faculty of Science, Osaka University, Toyonaka, Osaka 560-0043, Japan*
(Received 20 July 2004; revised manuscript received 12 October 2004; published 13 January 2005)

We report magnetic susceptibility and electrical resistivity measurements under hydrostatic pressure up to 2 GPa on single-crystalline $PrCu_2$, which exhibits the pressure-induced Van Vleck paramagnet-to-antiferromagnet transition at 1.2 GPa. The measured anisotropy in the susceptibility shows that the ordered $4f$ moments lie in the *ac* plane in the pressure-induced magnetic state. We propose that remarkable pressure effects on the susceptibility and resistivity are due to changes in the quadrupolar state of O_2^2 and/or O_2^0 under pressure. We present a simple analysis in terms of the singlet-singlet model.

DOI: 10.1103/PhysRevB.71.024408 PACS number(s): 75.30.Kz, 75.30.Cr, 71.70.Ej, 33.15.Kr

I. INTRODUCTION

Using a high-pressure technique, the volume and the corresponding properties of solids may be tuned, thereby inducing transformations from one solid state to another, as in the case of nonmagnetic-to-magnetic phase transitions and crystallographic phase transitions. In rare-earth compounds, the compression of the crystal modifies the electronic state through single-ion crystal-field and magnetoelastic interactions and/or interatomic interactions, such as quadrupolar coupling and the Ruderman-Kittel-Kasuya-Yoshida (RKKY) interaction mediated by conduction band electrons.[1] The orthorhombic $PrCu_2$ ($CeCu_2$ type of crystal structure) may be considered to be an exemplary compound in this respect. $PrCu_2$ has a singlet ground state and undergoes a cooperative Jahn-Teller (JT) transition at $T_{JT}=7.6$ K. The crystal field of local symmetry C_{2v} splits the full $^3H_4$ multiplet of Pr^{3+} into nine singlets. In fact, the magnetic susceptibility approaches a constant value at low temperature. As is mentioned below, a huge anisotropic magnetostriction[2] accompanies the metamagnetic transition, which occurs for the magnetic field applied parallel to the *ac* plane.[3,4] Consequently, considerable pressure effects on the magnetic state are expected in $PrCu_2$. In view of this, the effects of pressure on the magnetic susceptibility, specific heat, electric resistivity, and lattice constants were investigated recently.[5] A pseudouniaxial compression with compressibilities $\kappa_a \cong \kappa_c < \kappa_b$ is observed, but no signal of a structural transition is noted up to 4 GPa. However, at $P>1.2$ GPa, the susceptibility shows a remarkable maximum at $T=T_{max}$. At low temperature, an upturn in the specific heat developed with pressure, which can be attributed to the emergence of a spontaneous magnetic field. The estimated spontaneous fields are comparable to those in other magnetically ordered $4f$ electron systems.[5] Around a pressure of $P=1.2$ GPa, the resistivity at low temperatures is enhanced. These findings suggest that pressure-induced magnetism appears at $P>1.2$ GPa. In Fig. 1, we show the pressure-temperature ($P-T$) phase diagram of $PrCu_2$. The magnetic transition temperature (or T_{max}) increases steeply near 1.2 GPa and monotonously at higher pressure. At $P>1.7$ GPa, T_{max} becomes larger than T_{JT}, the latter being nearly pressure independent but exhibiting a weak maximum at $P=1.2$ GPa.[5]

This magnetic behavior is a reminder of the pressure-induced antiferromagnetism appearing at $P_c=3.0$ GPa (Ref. 6) in the cubic material PrSb, which is simply characterized by "induced-moment magnetism" (IMM). For the singlet ground state, no magnetic order develops when the interatomic exchange interaction K remains below a certain critical threshold K_c. For $K>K_c$, the so-called induced-moment transition occurs at finite temperature. However, when strong hyperfine interactions between nuclear and electronic moments exist, even for $K<K_c$, both moments can undergo a magnetic ordering at lower temperature.[1] In $PrCu_2$ at ambient pressure, actually, hyperfine coupled electron-nuclear magnetism (HCENM) appears at very low temperatures (i.e., below 54 mK).[1,7] Kawarazaki *et al.*[8] resolved the magnetic

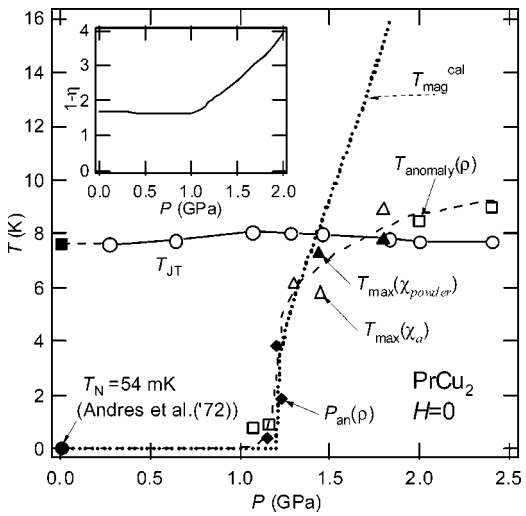

FIG. 1. Pressure-temperature phase diagram of $PrCu_2$ at $H=0$. The dotted line represents $T_{mag}^{cal}(P)$ calculated on the basis of the singlet-singlet model. $T_{max}(\chi_a)$, T_{max}(powder), and $P_{an}(\rho)$ were obtained previously in Ref. 5. The solid circle and square at $P=0$ were indicated in Refs. 7 and 4, respectively. Dashed and solid lines are guides for the eye. The inset shows the calculated enhancement factor as a function of pressure.

structure by neutron scattering. The electronic and nuclear spins on the Pr ion are sinusoidally modulated in magnitude with a modulation vector $\boldsymbol{Q_m}=(0.24,0,0.68)$ and point almost along the *a* axis. Consequently, it has been speculated that, in $PrCu_2$, the phase transition at $P=1.2$ GPa is of the HCENM-to-IMM.[5,9]

In the past decade, it has become clear that quadrupolar interactions play an important role in the magnetism in $PrCu_2$, especially, since the metamagnetic transition for magnetic fields in the *ac* plane is accompanied by very large magnetostrictions.[2–4] In addition to the crystal field interaction, the quadrupole-quadrupole couplings of $O_{xy}=J_x^2-J_y^2$ and $O_2^2=(2J_z^2-J_x^2-J_y^2)/\sqrt{3}$, where J_x, J_y, and J_z are angular moments, are essential for the reproduction of the features, such as, the cooperative JT and metamagnetic transitions, respectively.[4] The former is characterized as a ferroquadrupolar ordering of O_{xy}. On the other hand, the rotation of the quadrupolar moment of O_2^2 under a magnetic field is responsible for the latter. Unexpectedly, in $PrCu_2$ at $T=65$ K, magnetic ordering was observed by a comprehensive muon-spin-rotation/relaxation (μSR) study.[10] Spontaneous internal magnetic fields appear below 65 K. It is speculated that the magnetic structure is similar to that of the low-temperature HCENM phase at $T<54$ mK. The estimated ordered electronic moment of $0.29\mu_B$ is smaller than that of $0.54\mu_B$ quoted by Kawarazaki *et al.* It is suggested that a nonmagnetic interaction related to a collective state of O_{xy} is responsible for the magnetic ordering at $T<65$ K.

The magnetic state in the pressure-induced phase at $P>1.2$ GPa is not understood yet. In this work, we report a high-pressure study of the magnetic susceptibilities along the different crystal axes in order to characterize the magnetic structure at high pressure. Additionally, the electrical resistivity $\rho(T)$ is investigated down to 0.4 K in order to confirm the pressure-temperature ($P-T$) phase diagram and determine the effect of the pressure on the crystalline electric field splitting of the low-lying crystal field states. We found that, even in the paramagnetic region, the anomaly of the $\chi-P$ curve around $P_c=1.2$ GPa survives. This anomaly preceding the transition to the magnetic state is possibly related to the quadrupolar state at high pressure.

II. EXPERIMENTAL METHODS

Single-crystalline samples were made by a Czochralski pulling method in an induction furnace under a helium gas atmosphere.[3] The magnetization was measured at high pressure up to $P=1.8$ GPa using the Faraday method in the temperature range of 2–80 K. Measurements were done in a superconducting magnet system, which consists of a main solenoid coil producing a main field $\boldsymbol{H}_{\mathrm{main}}$ and a set of gradient coils located at the top and bottom sides of the main coil producing a field gradient, dH_z/dz along the vertical axis (the *z* axis) at the sample position. While supplying a current to the magnet coils, the force that is proportional to $\chi(\mathrm{d}H_z/\mathrm{d}z)H$ can be detected by the force balance. In contrast to the resistive magnet system, in which the magnetization $\boldsymbol{M}$ is perpendicular to the force $\boldsymbol{F}_z$, the superconducting magnet system produces $\boldsymbol{H}$ and $\boldsymbol{M}$ parallel to $\boldsymbol{F}_z$. In this configuration, it is possible to measure the anisotropy in the magnetization, since it is difficult for the easy axis of magnetization to rotate towards the direction of the magnetic field when the magnetization along the hard axis is measured.

The single-crystalline sample was put into a Teflon cell with Fluorinert as pressure-transmitting media. It was then pressurized in a piston-cylinder-type clamp made from a CuBe alloy. To obtain $\chi(T)$ in various magnetic fields and $T_{\max}$ and T_{JT}, we took data at $H=4$, 10, and 20 kOe. The resistivity was measured using a standard ac four-probe method using a Linear Research resistance bridge (model LR-700). In this case, a hybrid clamp cell made from NiCrAl and CuBe alloys, which can generate pressures over 2 GPa, was used. The sample was mounted on a specially designed plug and put inside a Teflon cell with the pressure-transmitting medium Flourinert.[5] The absorption pump-operated ^{3}He cryogenic system is described elsewhere.[11]

III. RESULTS AND DISCUSSION

A. Magnetic susceptibility

In Figs. 2(a)–2(c), we show the susceptibility under pressure for magnetic fields along the *a*, *b*, and *c* axes. Note that the applied magnetic field is well below the metamagnetic transition field $H_m>60$ kOe.[3] The susceptibility along the *a* axis $\chi_a(T)$ shows a pronounced maximum at $T_{\max}$ [Fig. 2(a)] for pressures $P>1.2$ GPa. In contrast, $\chi_b(T)$ shows no anomaly at $T_{\max}$ over the entire pressure range; however, a kink is observed at T_{JT}. For $\chi_c(T)$, the pressure-induced anomaly at $T_{\max}$ is less pronounced. The observed anisotropy in the susceptibility suggests that the ordered $4f$ moments lie in the *ac* plane, approximately parallel to the *a* axis. This is consistent with the observation that, at ambient pressure, the ordered nuclear and electronic moments are oriented approximately parallel to the *a* axis and sinusoidally modulated in magnitude below $T_{\mathrm{N}}=54$ mK.[8]

The JT-transition temperature as a function of pressure $T_{\mathrm{JT}}(P)$ can be obtained from the kink point of $\chi_b(T)$ [see inset of Fig. 2(b)]. T_{JT} depends weakly on pressure and exhibits a weak maximum at 1.2 GPa (Fig. 1). The pressure coefficients of T_{JT}, $(1/T_{\mathrm{JT}})dT_{\mathrm{JT}}/dP$, below and above 1.2 GPa, are 0.072 ± 0.01 and -0.043 ± 0.01 GPa^{-1}, respectively. On the other hand, $T_{\max}$ appears at 1.2 GPa and increases rapidly with pressure. It is important to note that T_{JT} is quite insensitive to pressure compared with $T_{\max}$. This supports the speculation that the quadrupolar state of O_{xy} is influenced slightly by the magnetic transition at $P>1.2$ GPa.

Figures 3(a)–3(c) show the pressure dependence of the susceptibilities along the *a*, *b*, and *c* axes, respectively, above and below T_{JT} measured in a field of $H=4$ kOe. $\chi_a(P)$ and $\chi_c(P)$ exhibit pronounced maxima around $P=1$ GPa in the lower temperature range, while $\chi_b(P)$ decreases linearly with pressure over the entire pressure range. This contrasting behavior between the pressure dependencies in the *ac* plane and the *b* axis seems to be in line with that observed in the dynamic phenomena of the quadrupolar moments that lie in the *ac* plane, as reported in Refs. 2–4. The linear thermal expansion coefficients α_a and α_c show anomalously sharp

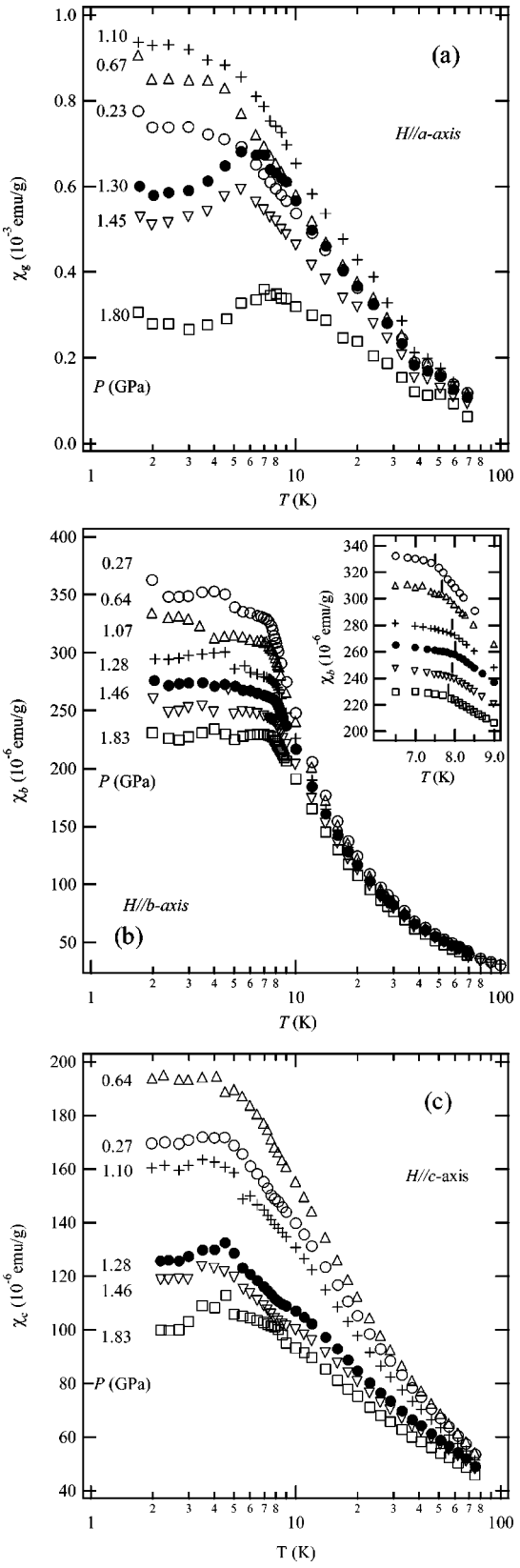

FIG. 2. Magnetic susceptibility of $PrCu_2$ as a function of pressure for applied magnetic fields parallel to the *a* (a), *b* (b), and *c* axes (c). The inset of (b) shows the Jahn-Teller-transition point as a function of pressure, determined by the kink in $\chi_c(T)$.

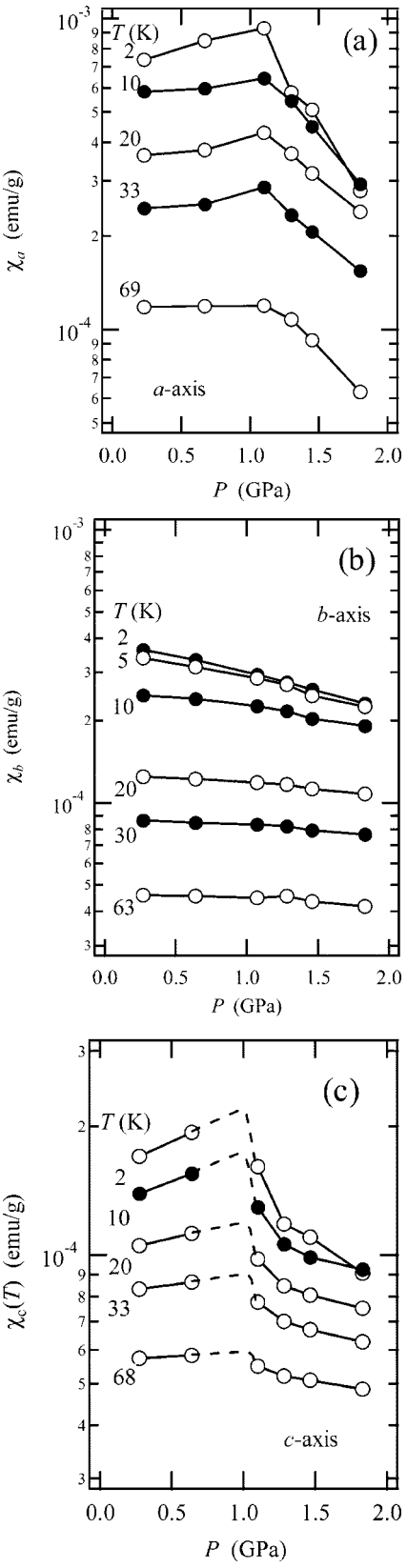

FIG. 3. (a)–(c) Pressure dependence of the magnetic susceptibility of $PrCu_2$ measured in a field of $H=4$ kOe directed along the *a*, *b*, and *c* axes, respectively, at various temperatures as indicated. Solid and dashed lines are guides for the eye.

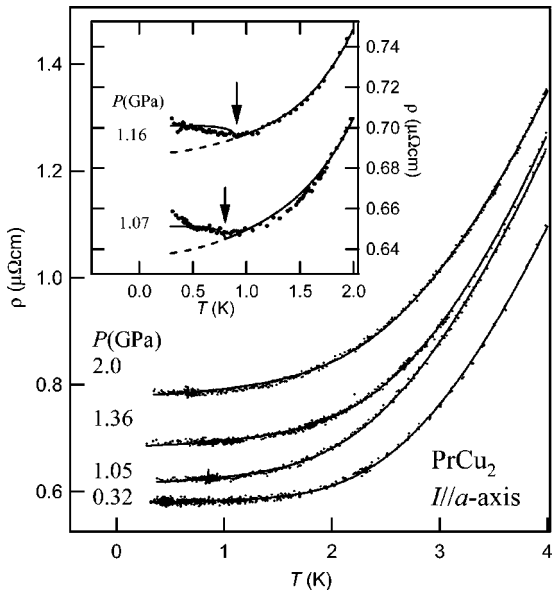

FIG. 4. Pressure variation of $\rho(T)$ at low temperatures for a current parallel to the a axis. The inset shows the upturn of $\rho(T)$ near $P=P_c$. Solid and dashed curves represent the calculated values based on Eqs. (2) and (1), respectively. See text for details.

peaks at T_{JT}, while α_b exhibits a weaker anomaly.[2] The metamagnetic behavior with the anomalously large magnetostriction occurs for the magnetic fields applied parallel to the *ac* plane.[3] It was confirmed that the easy (a) and the hard (c) axis directions of the magnetization interchange through the metamagnetic transition.[3,4] Based on a theoretical model including quadrupole-quadrupole interactions, it is derived that the cooperative JT transition results from a quadrupolar ordering of O_{xy}, while the metamagnetic transition is due to the rotation of the quadrupolar moment of O_2^2 under a magnetic field.[4] Namely, the quadrupolar state of O_2^2 is strongly coupled to magnetic moments in the *ac* plane but not considerably to that in the *b* axis; on the contrary, the JT transition considerably affects the magnetic moment in the *b* axis but not that in the *ac* plane, as shown in Fig. 2(b). It is likely, therefore, that the quadrupolar moments of O_2^2 and O_{xy} behave independently of each other under magnetic field. This situation is preserved also at high pressure. Notably, the maxima in $\chi_a(P)$ and $\chi_c(P)$ at around $P=1$ GPa are observed not only below but also well above T_{max} and T_{JT}, as shown in Figs. 3(a) and 3(c).

B. Electric resistivity and the singlet-singlet model

In Figure 4, we show $\rho(T)$ at various pressures. At low temperature ρ increases with pressure. Around $P=1$ GPa, a minimum in $\rho(T)$ is observed (see inset of Fig. 4). When plotted versus T^2 (Fig. 5), the low-temperature data clearly show that $\rho(T)$ deviates from the T^2 dependence with increasing temperature. In a previous paper, we claimed that the resistivity obeys the characteristics of the Fermi liquid $\rho(T)=\rho_0+AT^2$ down to 2 K.[5] This new result indicates that there is a thermally excited component in the resistivity due

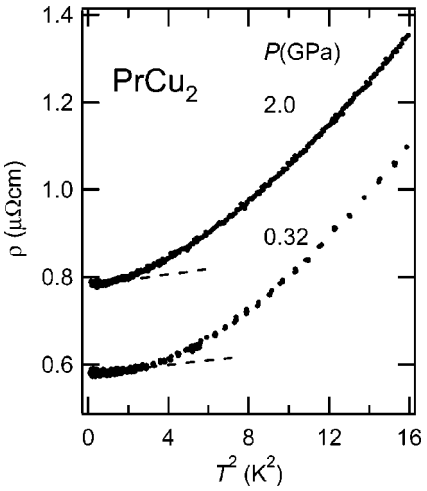

FIG. 5. Resistivity as a function of T^2 at various pressures. Note that $\rho(T)$ deviates clearly from a T^2 law (dashed lines) with increasing temperature.

to the low-lying excitations in the crystal field states of $PrCu_2$.

In order to obtain information about the crystal field splitting in $PrCu_2$ from the $\rho(T)$ data, we fitted the data below 4 K to the following simple equation:

$$\rho(T)=\rho_0+AT^2+\sum_i \rho_i \frac{\exp(-\Delta_i/k_BT)}{\sum \exp(-\Delta_i/k_BT)}. \qquad (1)$$

Here, the fitting parameters are the residual resistivity ρ_0, the coefficient of the T^2 term A, a component of the thermally excited state in the resistivity ρ_i, and the corresponding crystal field splitting Δ_i. The third term yields the contributions from thermally excited singlet states. We assume that ρ_i is independent of the temperature. Based on the crystal field level scheme for the four lowest levels, as shown in Fig. 6,[12] we have ρ_1, $\rho_2 \ll \rho_3$ at the lowest pressure. This result makes plausibly that the singlet-singlet model with the ground and the third excited states describes the low-temperature resistivity. Otherwise, the first and second excited states respond mainly to the JT transition, as noted previously.[13]

Figures 7(a) and 7(b) show the fitting parameters as a function of pressure obtained on the basis of the singlet-singlet model. As previously indicated,[5] ρ_0 and A are enhanced anomalously at P_c and increase with pressure above P_c, while both $\rho_1(P)$ and $\Delta(P)$ seem to have a weak minimum at P_c. Remarkably, the extrapolated value of $\Delta \sim 14$ K at $P=0$ corresponds well with the energy splitting

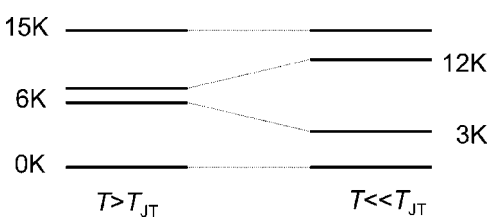

FIG. 6. The low-lying crystal field states in $PrCu_2$ at $T>T_{\mathrm{JT}}$ and $T \ll T_{\mathrm{JT}}$ according to Ref. 12.

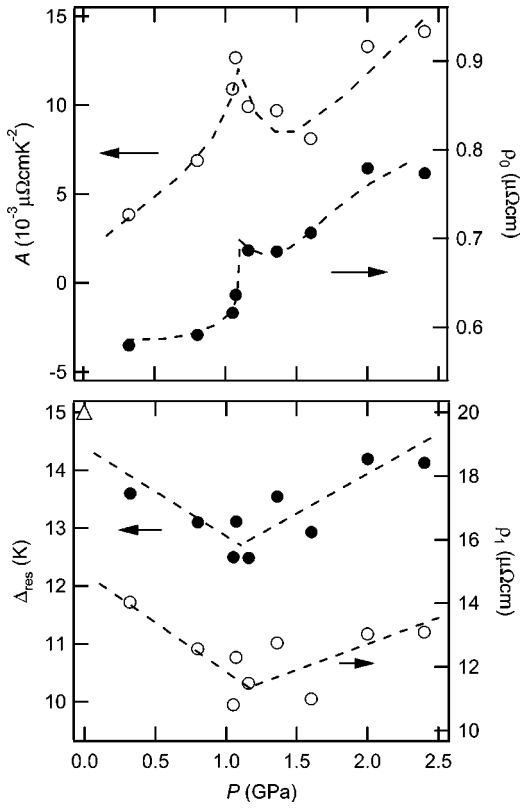

FIG. 7. Fitting parameters (a) A and ρ_0, (b) Δ and ρ_1 as a function of pressure. Dashed lines are guides for the eye. The data point (triangle) at $P=0$ is obtained from inelastic neutron scattering experiments (Ref. 12).

between the ground and the third excited states obtained from inelastic neutron scattering experiments.[12] Kawarazaki *et al.*[13] measured the anisotropy and the dispersion of the singlet-singlet crystal-field exciton down to 1.8 K in $PrCu_2$. The excitons with J_x polarization and those with J_y polarization have quite different dispersions. The strong dispersive J_x transition shows a substantial softening of the excitation energy at $\boldsymbol{Q}_m = 0.24\boldsymbol{a}^* + 0.68\boldsymbol{c}^*$. This is consistent with the observation that the ordered magnetic moment is parallel to the a axis.[8] As mentioned above, it is plausible that the magnetic structure at $P=0$ is preserved in the pressure-induced phase. Additionally, anisotropic RKKY interactions between the $4f$ electrons $K_{a,b,c}$ have been reported.[13] The low-lying crystal-field splitting is not sensitive to the application of hydrostatic pressure in $PrCu_2$, as shown in Fig. 7(b). Therefore, we suggest that the anisotropic pressure dependence of the susceptibilities $\chi_{a,b,c}$ for the most part, result from the anisotropy in the exchange interactions $K_{a,b,c}$.

Around P_c, $\rho(T)$ obviously exhibits a hump at low temperature, as shown in the inset of Fig. 4. Such an increase is also observed at an antiferromagnetic transition due to the opening of an energy gap at the Fermi surface.[14] In this case, the resistivity, $\rho'(T)$, can be written as

$$\rho'(T) = \frac{\rho(T)}{1 - gm(T)}, \tag{2}$$

where $\rho(T)$ is the resistivity of the normal state and g is a truncation factor. $m(T)$ is defined as $M_Q(T)/M_Q(0)$, where $M_Q(T)$ is the staggered moment and is approximately expressed as $m(T)=[1-(T/T_N)^2]^{1/2}$. In the inset of Fig. 4, the calculated ρ in the vicinity of P_c is shown together with the experimental data. The structure with a minimum in $\rho(T)$ is reproduced. At $P>1.9$ GPa, the hump in $\rho(T)$ is observed, which can be reproduced by Eq. (2), whereas the $\rho(T)$ data is not shown here. The truncation factor g is obtained to be 0.02-0.03, which is considerably smaller than the values 0.5–0.6 obtained for the spin density wave (SDW) transition in Cr and related compounds.[14] This suggests that the low-lying crystal field states of the $4f$ electrons are weakly hybridized with the conduction electrons. The anomalous points associated with the pressure-induced transition in $\rho(T)$, T_{anomaly}, are shown as a function of pressure in Figs. 1 and 9(a).

C. Analysis based on the singlet-singlet model

In this section, we investigate to what extent the singlet-singlet model can reproduce the pressure-temperature phase diagram of $PrCu_2$ shown in Fig. 1. Before we calculate the magnetic transition temperature as a function of pressure, we recall a simple model for a Van Vleck paramagnet with a singlet ground state and the first excited singlet state located at an energy Δ, the so-called singlet-singlet model. The interaction between the electronic and nuclear magnetic moments is ignored. In this model, the magnetic phase diagram is determined as a function of a characteristic factor $\eta = 4K_0\alpha^2/\Delta$ where K_0 and α are the interatomic electronic exchange interaction and the off-diagonal matrix element of J_z between the two singlets $<0|J_z|1>$, respectively. It is derived that the magnetic order and a spontaneous moment appear abruptly at the critical points $|\eta|=1$ in an accessible temperature range.[1,9] It was shown in Ref. 5 that, in $PrCu_2$, the characteristic parameter η reaches the critical value $|\eta_c| = 1$ at $P=1.2$ GPa. However, this previous estimate depended strongly on the initial value of $\eta(0)$. Since the value $\eta(0)$ in $PrCu_2$ is controversial,[7,11] we assume the condition $|\eta_c|=1$ at $P=1.2$ GPa in the following. In the singlet-singlet model, the susceptibility at $T \ll \Delta/k_B$ is expressed as

$$\chi(0) = \frac{c}{\Delta}\frac{1}{1-\eta}, \tag{3}$$

where c is pressure independent. Consequently, the pressure coefficient of χ consists of the following two terms:

$$\frac{1}{\chi(0)}\frac{d\chi(0)}{dP} = \frac{d\ln\chi(0)}{dP} = -\frac{d\ln\Delta}{dP} - \frac{d\ln(1-\eta)}{dP}. \tag{4}$$

The first term accounts for the crystal-field splitting and the second term is due to the enhancement factor $1-\eta$. In the present case, η is negative (antiferromagnetic). To compare the first and the second terms in Eq. (4), $\Delta(P)$ obtained above from the $\rho(P,T)$ data and $\chi_a^{-1}(P)$ are shown in a logarithmic-linear plot (Fig. 8). Note that, in the figure, the gradients of Δ and χ_a^{-1} with respect to pressure correspond with the respective pressure coefficients. The signs of $d\ln\Delta/dP$ and $d\ln\chi_a/dP$ change abruptly at P_c. From

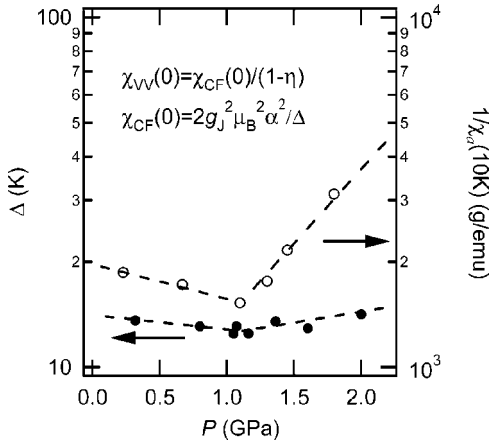

FIG. 8. $\Delta(P)$ and $\chi_a^{-1}(P)$ in a log-lin plot. Dashed lines are guides for the eye.

Eq. (4) and the values of $d\ln\Delta/dP=0.10\pm0.03$ and $d\ln\chi_a/dP=-1.05\pm0.07$ GPa^{-1}, it is derived that $d\ln(1-\eta)/dP=0.95\pm0.07$ GPa^{-1}, which is much larger than $d\ln\Delta/dP$ at $P\geqslant P_c$. Using the values of $d\ln\chi a/dP$ just above $T_{\max}$ and $d\ln\Delta/dP$, we numerically estimated the transition temperature $T_{\mathrm{mag}}^{\mathrm{cal}}(P)$. The results are shown in Fig. 1, which reveals that the calculated $T_{\mathrm{mag}}^{\mathrm{cal}}(P)$ increases more rapidly with pressure than the experimental value. On the contrary, below P_c, the pressure coefficient of $d\ln(1-\eta)/dP=0.15\pm0.03$ GPa^{-1} derived from the experimental values $d\ln\Delta/dP=-0.08\pm0.03$ and $d\ln\chi_a/dP=0.23\pm0.03$ GPa^{-1}, is comparable with $d\ln\Delta/dP$. Consequently, the pressure coefficient of not only Δ but also the antiferromagnetic exchange coupling K_a changes abruptly at P_c. Using the pressure coefficients of the enhancement factor $1-\eta$ above and below 1.2 GPa and the initial value of $\eta(0)=-0.8$ used in Ref. 5, we also calculated the pressure dependence of $1-\eta$, shown in the inset of Fig. 1. Below 1.2 GPa, the enhancement factor is nearly constant, but it increases rapidly above 1.2 GPa. The magnitude of the antiferromagnetic exchange coupling along the a axis K_a increases anomalously with pressure at the induced-moment transition.

D. Magnetic and quadrupolar phase diagrams

Figures 9(a) and 9(b) show the magnetic and the quadrupolar transitions in the $P-T$ phase plane, respectively. In these figures, the points at which $\chi_a(P)$ exhibits a maximum are connected by the dotted line, which is denoted as $P_{\max}$. In the magnetic phase diagram [Fig. 9(a)], the $P_{\max}-T$ curve seems to make a special point at $(P_c,T_c)\approx(1.2\ \mathrm{GPa},5\ \mathrm{K})$ with the $T_{\max}-P$ curve. At lower pressure, it is likely that $T_{\max}(P)$ extends to the point, $T_N=54$ mK at $P=0$. This is supported by the fact that the magnetic structure at higher pressure is similar to that at $P=0$, as mentioned above. $T_{\max}(P)$ increases rapidly along with the $T_{\max}-P$ curve, deviates from it, and moderately increases with pressure [Fig. 9(a)]. Figure 9(b) shows $T_{\mathrm{JT}}(P)$ at $H=0$ with the quadrupolar states of $\langle O_2^2\rangle$ and $\langle O_{xy}\rangle$ derived by comprehensive experimental and theoretical studies at ambient pressure.[4]

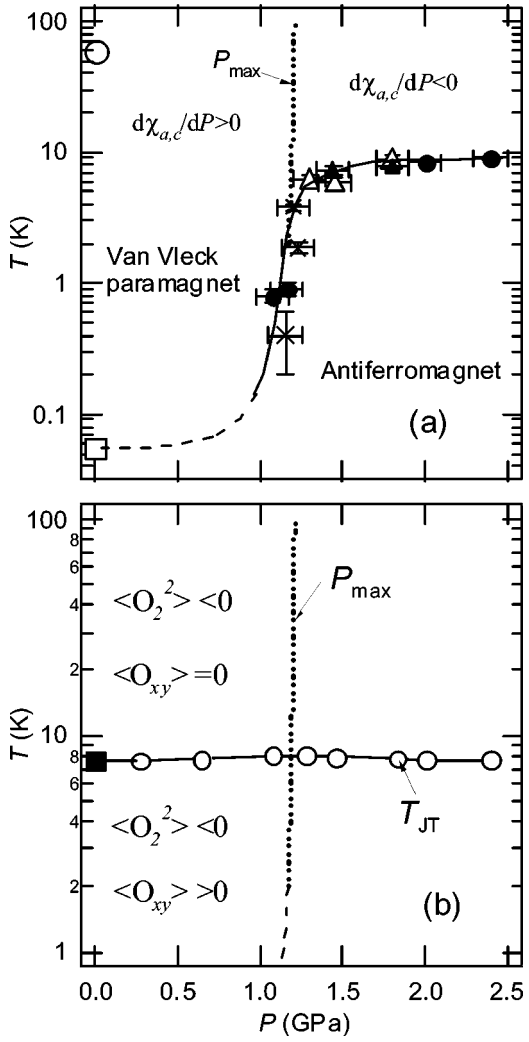

FIG. 9. Proposed magnetic (a) and quadrupolar (b) phase diagrams of $PrCu_2$ at $H=0$. The solid, dotted, and dashed lines are guides for the eye. The circle and square at $P=0$ indicate the transition temperatures obtained in Refs. 10 and 7, respectively. The states of O_{xy} and O_2^2 at $P=0$ are derived in Ref. 4.

As mentioned above, the quadrupolar states of O_2^2 and O_{xy} are strongly coupled with magnetic moments in the *ac* plane and the *b* axis, respectively, and behave quite independently of each other. This fact is reflected into the anisotropic magnetic behaviors indicated under pressure. The pressure-induced magnetism is not simply characterized as an induced-moment transition. Actually, the anomalous changes of Δ and $1-\eta$ accompanying the pressure-induced magnetic transition around $P=1.2$ GPa have been indicated. At ambient pressure, despite the paramagnetic state, the $4f$ moment exhibits metamagnetism due to the collective response of the ordered O_2^2 moment with respect to the external magnetic field. In the same way, if we assume that the magnetic anomaly at $P_{\max}$ is due to a collective response of the ordered O_2^2 moment under external pressure, it is plausibly explained that $\chi_{a,c}(P)$ exhibits the anomalous maximum and, on the contrary, $\chi_b(P)$ has no anomaly in the paramagnetic region.

Finally, it is noteworthy that the anisotropic compression under hydrostatic pressure, $\kappa_a \cong \kappa_c < \kappa_b$,[5] corresponds effectively with the symmetry strains, $\varepsilon_u = (2\varepsilon_{zz} - \varepsilon_{xx} - \varepsilon_{yy})/\sqrt{3}$ and $\varepsilon_v = \varepsilon_{xx} - \varepsilon_{yy}$, which couple to the quadrupolar moments O_2^0 and O_2^2, respectively, via the magnetoelastic interaction formulated with terms such as $G_v \varepsilon_v O_2^2$, where G_v is the magnetoelastic coupling constant.[15] The uniaxial tendency of the compression may stabilize or destabilize the component of O_2^0 and/or O_2^2 in the ordered quadrupolar state but affect the O_{xy} state only weakly. Similar to the case of the $H-T$ phase diagram, the complexity of the $P-T$ one results not only from the IMM in the Van Vleck magnet but also from the couplings involved with the quadrupolar moments, which are generally known as a hidden order parameter that has a considerable effect on the magnetic exchange interaction between the neighboring $4f$ moments and, hence, the magnetic grand state.[15]

IV. SUMMARY

We have reported the susceptibility and transport data of single-crystalline $PrCu_2$ under pressure. The observed anisotropy in the susceptibility indicates that, below the pressure-induced magnetic transition, the ordered moments lie in the *ac* plane. In the investigated temperature range, $2\ \mathrm{K} < T < 80\ \mathrm{K}$, a magnetic anomaly at P_c is observed for magnetic fields directed in the *ac* plane, while no anomaly results for magnetic fields along the *b* axis. Near P_c, the resistivity data show an anomaly as a function of temperature near 0.8 K and above T_{JT}. The singlet-singlet model can only in part account for the observed phase diagram. Our new results lead us to speculate the pressure-induced anomaly of susceptibility at $P \sim 1.2$ GPa above the magnetic transition appears as a precursor of the pressure-induced magnetism. Further investigation with respect to the magnetic and quadrupolar states should be done on a microscopic basis, e.g., neutron diffraction and μSR measurements under high pressure.

*E-mail address: NAKA. Takashi@nims.go.jp

[1] K. Andres and O. V. Lounasmaa, *Progress in Low Temperature Physics*, edited by D. F. Brewer (North-Holland, Amsterdam, 1982), Vol. 8, Chap. 4.
[2] T. Takeuchi, P. Ahmet, M. Abliz, R. Settai, and Y. Ōnuki, J. Phys. Soc. Jpn. **65**, 1404 (1996).
[3] P. Ahmet, M. Abliz, R. Settai, K. Sugiyama, Y. Ōnuki, T. Takeuchi, K. Kindo, and S. Takayanagi, J. Phys. Soc. Jpn. **65**, 1077 (1996).
[4] R. Settai, S. Araki, P. Ahmet, M. Abliz, K. Sugiyama, Y. Ōnuki, Terutaka Goto, H. Mitamura, Tsuneaki Goto, and S. Takayanagi, J. Phys. Soc. Jpn. **67**, 636 (1998).
[5] T. Naka, J. Tang, J. Ye, A. Matsushita, T. Matsumoto, R. Settai, and Y. Ōnuki, J. Phys. Soc. Jpn. **72**, 1758 (2003).
[6] D. B. McWhan, C. Vettier, R. Youngblood, and G. Shirane, Phys. Rev. B **20**, 4612 (1979).
[7] K. Andres, E. Bucher, J. P. Maita, and S. A. Cooper, Phys. Rev. Lett. **28**, 1652 (1972).
[8] S. Kawarazaki and J. Arthur, J. Phys. Soc. Jpn. **57**, 1077 (1988).
[9] T. Murao, J. Phys. Soc. Jpn. **31**, 683 (1971); **33**, 33 (1972).
[10] A. Schenck, F. N. Gygax, and Y. Ōnuki, Phys. Rev. B **68**, 104422 (2003).
[11] K. Bakker, Ph.D. Thesis, University of Amsterdam, 1993.
[12] J. K. Kjems, *Electron Phonon Interaction and Phase Transition*, edited by T. Riste (Plenum Press, New York, 1977), p. 302.
[13] S. Kawarazaki, Y. Kobashi, M. Sato, and Y. Miyako, J. Phys.: Condens. Matter **7**, 4051 (1995).
[14] S. Maki and K. Adachi, J. Phys. Soc. Jpn. **46**, 1131 (1979).
[15] T. Yanagisawa, T. Goto, Y. Nemoto, S. Miyata, R. Watanuki, and K. Suzuki, Phys. Rev. B **67**, 115129 (2003).